

# Berry's Phase and Fine Structure

BERND BINDER<sup>1</sup>

Date: 25.7.2002

## Abstract

Irrational numbers can be assigned to physical entities based on iterative processes of geometric objects. It is likely that iterative round trips of vector signals include a geometric phase component. If so, this component will couple back to the round trip frequency or path length generating a non-linear feedback loop (i.e. induced by precession). In this paper such a quantum feedback mechanism is defined including generalized fine structure constants in accordance with the fundamental gravitomagnetic relation of spin-orbit coupling. Supported by measurements, the general relativistic and topological background allows to propose, that the deviation of the fine structure constant from  $1/137$  could be assigned to Berry's phase. The interpretation is straightforward: spacetime curvature effects can be greatly amplified by non-linear phase-locked feedback-loops adjusted to single-valued phase relationships in the quantum regime.

## Introduction

A quantum mechanics of spin can not be complete without considering the phase evolution of a wave function including interference phenomena and geometric spin precession. Berry's phase [1] can appear in purely classical situations such as round trip excursions on curved surfaces. Since spatial phases appear in any kind of wave propagation, different manifestations of this extremely general phenomenon have been found in several branches of physics from the high energy regime to the low. In addition to a Hamiltonian-induced dynamic phase, a quantum state evolving in parameter space on a trajectory that returns to the initial state acquires an extra phase termed geometric phase. This additional phase or angle depends only on the geometry of the Hamiltonian's trajectory through parameter space and not on its time evolution. Various manifestations of geometric phases exist and are connected with names like Aharonov, Anandan, Berry, Bohm, Pancharatnam, Simon, Thomas, Wilczek and many others, see e.g. [2]. Although there are no widely recognized practical applications of the nonabelian gauge theory, its experimental observations have been reported in many fields of science. But quantum electrodynamics (QED) was established long before Berry's phase was discovered. The successful concept of QED is perturbative and based on powers of the coupling constant  $\alpha$ . QED handles (hyper)fine structure, Lamb shift, spin anomalies at the most accurate level while ignoring Berry's phase. A quick search for Berry in this context over the last 10 years in a physics archive returns almost no hits. The situation is probably unbalanced regarding the connections of Dirac's theory and Berry's phase. Dirac's equation and Dirac's theory of monopoles [3] are very important for the foundations of QED especially in the atomic range. A magnetic monopole as a logical consequence of the Dirac theory is necessary to quantize charge. Berry's phase is intimately related to Dirac magnetic monopoles and arises naturally in the field of a monopole [1]. But magnetic monopoles have a similar status like Berry's phase: an abstract geometrical and topological feature, where the topological structure of this abstract manifold is under special circumstances observable and physical. But no monopole has been found, at least not identified. This fact and the rather exotic status seems to imply for many scientists that Berry's phase could have no big impact on the foundations of quantum mechanics manifested,

---

<sup>1</sup>email: binder@quantics.com, Weildorferstr.22, 88682 Salem-Neufrach, Germany ©2002

i.e. in atomic spectra.

But arguments that support the role of geometric phases in atomic physics can be found regarding the fine and hyperfine structure, since transitions in this range (GHz, atomic clocks) depend on exact frequency and phase relationships. These clocks usually depend on phase-locked loops, where phase factors or phases representing the ‘holonomy’ provide for important boundary conditions while reducing the degree of redundancy in variables. Usually, controlled by external fields, the geometric phase has a passive role, but in a phase-locking process the geometric phase could also couple back to the dynamic phase. Consequently, it is very interesting to consider round trips of vector signals additionally constrained by an emerging geometric phases.

## Generalized Berry phase

The non-adiabatic generalization of [4] defines a geometric phase factor for any cyclic evolution of a quantum system (experimentally verified e.g. in [5]). Consider a  $T$ -periodic cyclic vector  $|\psi(\tau)\rangle$  that evolves on a closed path  $\mathcal{C}$  according to

$$|\psi(T)\rangle = e^{i\varphi(T)} |\psi(0)\rangle, \quad (1)$$

where the total phase  $\varphi(T)$  acquired by the cyclic vector can naturally be decomposed into a geometric  $\varphi_g(T)$  and dynamical phase  $\varphi_d(T)$

$$\varphi(T) = \varphi_g(T) + \varphi_d(T). \quad (2)$$

The dynamical phase for one loop  $t \in [0; T]$  is with the Schrödinger equation given by

$$\varphi_d(T) = -\frac{1}{\hbar} \int_0^T \langle \psi(\tau) | H(\tau) | \psi(\tau) \rangle d\tau. \quad (3)$$

The Berry phase or geometric phase depends not on the explicit time dependence of the trajectory and is for one loop given by

$$\varphi_g(T) = i \oint_{\mathcal{C}} \langle \psi(\tau) | d | \psi(\tau) \rangle. \quad (4)$$

The ‘parallel transported’ spin vector will come back after every loop with a directional change  $\varphi_g(T)$  equal to the curvature enclosed by the path  $\mathcal{C}$ . On the unit sphere the curvature increment is proportional to the area increment that can be a spherical triangle with area given by

$$d\Omega := [1 - \cos \theta(\tau)] d\varphi(\tau), \quad (5)$$

the total area enclosed by the closed orbit (loop) is equal to

$$\Omega = \oint_{\mathcal{C}} d\Omega := \int_0^T d\tau [1 - \cos \theta(\tau)] \dot{\varphi}(\tau). \quad (6)$$

The Berry phase  $\varphi_g(T) = J\Omega$  and the total phase are proportional to spin  $J$ . In the standard case of precession on the sphere

$$\varphi_g(T) = 2\pi J(1 - \cos \theta), \quad \varphi(T) = 2\pi J, \quad (7)$$

where  $\theta$  is the vertex cone semiangle,  $\varphi(T) = 2\pi J$ ,  $\varphi_d(T) = 2\pi J \cos \theta$ . With  $n$  parameters  $\lambda_i(t)$ ,  $i = 1, 2, \dots, n$  that span a closed curve  $\mathcal{C}$  in the  $T$ -periodic parameter space  $\lambda_i(0) = \lambda_i(T)$ , the Berry phase may be represented in terms of the ‘gauge potential’

$$A_i = i \langle \psi | \frac{\partial}{\partial \lambda_i} | \psi \rangle, \quad (8)$$

$$\varphi_g(T) = \oint_{\mathcal{C}} A = \int_{\mathcal{S}_{\mathcal{C}}} F, \quad F = dA, \quad (9)$$

where  $A$  can be regarded as a winding number density,  $\mathcal{S}_{\mathcal{C}}$  is an arbitrary surface in the parameter space bounded by the contour  $\mathcal{C}$ . For more details regarding monopoles and Wilson loops on the lattice in non-Abelian gauge theories, see e.g. [6]. Note if the Berry phase contains a string-like singularity (Dirac string) somewhere on the surface of  $\mathcal{S}$ , the position of the singularity may be arbitrary shifted by U(1) gauge transformations. In the first step we will introduce a simple feedback relation of the geometric phase to the dynamical phase.

### Spin-orbit feedback loop

The mostly important question is, what balances both parts of the total phase, what is the phase boundary condition? It is likely that iterative round trips of vector signals include a geometric phase component. If so, this component will couple back to the round trip frequency or path length generating a non-linear feedback loop (i.e. induced by precession). A ‘rolling cone’ representing a vector state or signal is probably the simplest model of spin-orbit coupling. Rotated once, the cone will change its orbital orientation by a special angle, rotated  $M$ -times in the quantum case, the cone will return to the initial position with integral  $M$  (providing for single-valuedness). But precession will change the path of the rolling cone such, that the number of conic sub-loops and the effective orbital frequency and radius are changed. This is a non-linear feedback situation, since a change in the number of loops couples back to the geometric and dynamical phase.

Starting with this model,  $M$  can divide the total phase range into  $M$  sub-loop intervals  $\Delta\varphi(T) = \Delta\varphi_d(T) + \Delta\varphi_g(T)$  where

$$\varphi_d(T) = M\Delta\varphi_d(T), \quad \varphi_g(T) = M\Delta\varphi_g(T). \quad (10)$$

Precession can be interpreted as a phase modulation of the orbital path length and could couple to the number of sub-loops by modulating the ‘rolling cone path’. It is very likely, that one or more extra loops with range  $\Delta\varphi_d(T)$  fit by an integral quantum number  $M_g$  within one vertex cone range  $2\theta$  providing for the feedback relation

$$2\theta = M_g\Delta\varphi_d(T). \quad (11)$$

This is an orbital resonance condition regarding the dynamical phase and the precession phase, in the next sections we will analyze also a radial resonance of the geometric phase with the precession phase, see fig.1. Now it is possible to find with eq.(7), eq.(10), and eq.(11) the optimum  $\theta$  for a given  $M$  and  $J$ , where

$$M\theta = JM_g\pi \cos \theta. \quad (12)$$

As a test for  $J = M_g = 1$  and  $M > 0$ , eq.(12) can be solved by iteration

$$\theta_{i+1} = \frac{\pi \cos \theta_i}{M}. \quad (13)$$

After a few steps the algorithm converges (no problem for  $JM_g \ll M$ ). Since  $M_g$  contributes to the total number of sub-loops units one could write  $M = M_d + M_g = \pm 1, \pm 2, \dots$ . Now  $M$  contains two parts:  $M_d$  counts the sub-loops that contribute to the dynamical phase for one circular loop over the phase range  $2\pi$ , while  $M_g = \pm 1, \pm 2, \dots$  counts the extra number of sub-loops induced by precession at vertex semiangle  $\theta > 0$ . Consequently,  $M_g$  stands for the geometric contribution or loop/sub-loop interaction. Requiring single-valuedness all three numbers will be integer.

The criterion for the convergence of the nonlinear affine iterative system or the asymptotic stability of the fixed point will be visualized in the next sections showing bifurcations and unstable regimes.

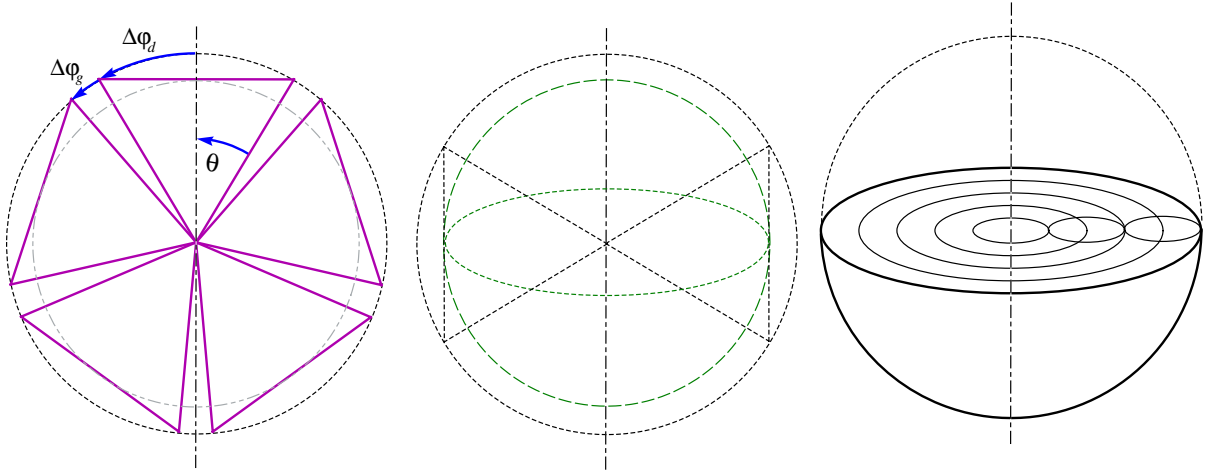


Figure 1: On the left the orbital resonance of dynamical phase and precession angle (for  $M = 5$  and  $M_g = J = 1$ ), in the middle the effective frequency change, and on the right the radial resonance of geometric phase and precession angle (quantum number  $N$ ).

### Generalized fine structure constants

The coupling must be proportional to the dynamical part of the phase interval  $\Delta\varphi_d(T)/\varphi(T)$  and to spin  $J$ . Therefore, generalized fine structure constants can be defined by

$$\alpha(M) = \frac{J\Delta\varphi_d(T)}{\varphi(T)} = \frac{J\varphi_d(T)}{M\varphi(T)}. \quad (14)$$

With eq.(10) and eq.(14), in eq.(2)

$$\frac{\varphi_g(T)}{2\pi J} = 1 - \frac{M\alpha}{J}, \quad (15)$$

the dynamical part of eq.(15) with eq.(14) in eq.(7) provides for

$$M\alpha = J \cos(\theta). \quad (16)$$

Comparing eq.(12) with eq.(16) the precession cone vertex angle  $2\theta$  of eq.(7) equals the dynamical phase of the spin-orbit interaction part in eq.(10) with

$$\theta = \pi M_g \alpha. \quad (17)$$

The two possible signs can be combined to  $M/M_g > 0$

$$M\alpha = J \cos(\pi M_g \alpha), \quad (18)$$

and for  $M/M_g < 0$

$$M\alpha = J \cos(\pi - \pi M_g \alpha). \quad (19)$$

Results for  $\alpha$  with variable  $M$  for  $M_g = J = 1$  are shown in table 1 and visualized in fig.1 and [7]. For a geometric phase contribution  $\Delta\varphi_g(T) > 0$  one can expect  $\alpha < J/M$ . This adjusts the precession cone angle to the  $M$ -periodic orbit where (a) the effective radius is changed and (b) the number of rolling cycles is changed by  $M_g$ . The resulting non-linear affine iteration system can be used to find  $\alpha$  by converging towards an optimum or show instabilities and chaotic behavior with bifurcations.

Table 1:

Convergent fine structure (re)generation constants  $\alpha$  for  $Z_e = 1$  and variable  $M > 2$ . The third row shows  $N = |\Delta\varphi_d(T)/\Delta\varphi_g(T)|$  or  $|N_{\pm}|$  (bottom), known as winding number on helical paths.

$M$	$J/\alpha$	$N$
3	4.13669	2.63924
4	4.96178	4.15896
5	5.82662	6.04873
6	6.72097	8.32214
7	7.6371	10.98727
137	<b>137.03600941164</b>	3804.560912
137	<b>137.03600998817</b>	3804.5 <sup>1</sup>
137	<b>137.03600052556</b>	3805.5 <sup>1</sup>
137	<b>137.03599106791</b>	3806.5 <sup>1</sup>
137	137.03598161523	3807.5 <sup>1</sup>

<sup>1</sup> The next hypocycloidal or epicycloidal resonances for  $M = 137$  (see fig.2, eq.(26)) instead of free running ratio  $N$  between dynamical and geometric phase.

## Gravitomagnetic coupling

The bridge to general relativity has already been built in the previous sections by calculating the geometric phase via ‘parallel transport’ on a curved surface. Let  $\omega_M$  be the orbital frequency of a quantum particle on a circular path. The spin-rotation coupling will act on the particle with mass-energy  $E$  and Compton wavenumber  $k = E/\hbar c = \omega/c$  by generating precession at frequency  $\omega_p = E_p/\hbar$  and energy  $E_p$ . The fine structure constants eq.(14) and relative dynamical coupling strengths can be defined by

$$\alpha = \frac{J\omega_M}{\omega}, \quad (20)$$

a typical ratio orbital frequency divided by a Compton frequency with particle spin  $J$ . If precession as a frequency ratio is related to a geometric phase

$$\frac{\omega_p}{\gamma\omega} = \frac{\varphi_g(T)}{2\pi J}, \quad (21)$$

and the coupling part to a dynamical phase according to eq.(15) and eq.(20), the general expression for spin-rotation coupling observed in the laboratory frame (relativistic correction  $\gamma$ ) can be assumed to be

$$\frac{\omega_p}{\gamma\omega} = 1 - M \frac{\omega_M}{\omega}, \quad (22)$$

or

$$E_p = \gamma(E - M\hbar\omega_M), \quad (23)$$

a form that corresponds exactly to the gravitomagnetic spin-rotation coupling of Mashhoon [8], a Lense - Thirring effect [9] (also in [10, 11]), where an integer  $M$  covers scalar and vector fields. Usually, the gravitomagnetic effect can be hardly observed because of its tiny magnitude (tests with orbiting gyroscopes are on the way, see gravity probe B news [12]). But the tiny magnitude of the gravitomagnetic field in a classical measurement does not necessarily mean, that the magnitude of the emerging geometric phase and related quantum mass-energy currents in feedback loops must be tiny. Recently, [13] discussed coupling gravitomagnetism-spin and Berry's phase and pointed out, that the geometric phase changes should depend exclusively upon the solid angle of a field, and not on the strength of the field. If gravitomagnetic spin-rotation coupling eq.(23) controls the feedback loop in combination with eq.(18), the mass-energy current could increase to a level that is only limited by damping and (multipole) radiation effects, probably a level characterized by electromagnetism.

In this context there are some noteworthy comments from Mashhoon:

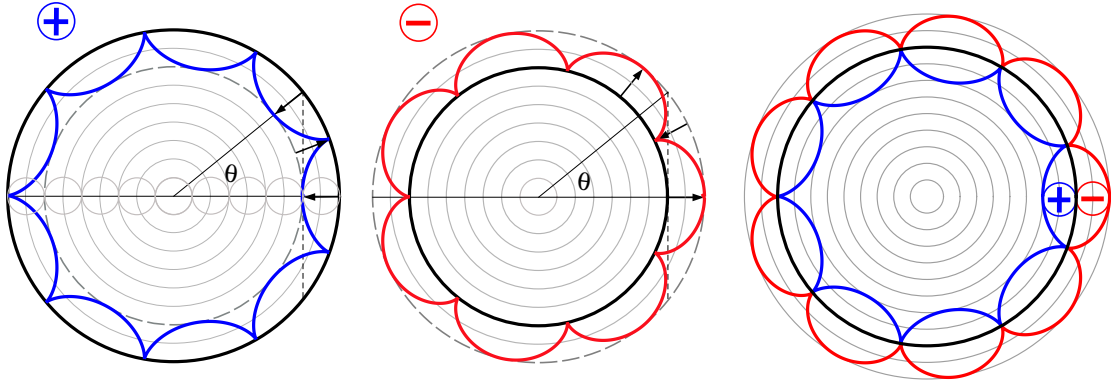


Figure 2: The geometric and dynamic phase evolution at resonance: on the left hypocycloids  $N_+ = 4.5$  ( $N = 4$ ), in the middle epicycloids with  $N_- = -3.5$  ( $N = 4$ ). On the right both are adjusted with  $N_+ = 4.5$  ( $N = 4$ ) and  $N_- = -4.5$  ( $N = 5$ ), but in this case epicycloids and hypocycloids have different radii.

The coupling of intrinsic spin with rotation reveals the rotational inertia of intrinsic spin. The phase perturbation arising from spin-rotation coupling can be developed as a natural extension of the celebrated Sagnac effect [10]. Spin-rotation coupling, however, violates the underlying assumption of locality in special relativity: that the results of any measurement performed by an accelerating observer (in this case the measurement of frequency) are locally equivalent to those of a momentarily comoving inertial observer, but agrees with an extended form of the locality hypothesis. This is a nontrivial axiom since there exist definite acceleration scales of time and length that are associated with an accelerated observer [10].

Note, that orbital precession of the geometrical phase provides for a change in the frequency ratio

$$\frac{\omega}{M\omega_M} = \frac{1}{\cos\theta} = \frac{\varphi_d(T) + \varphi_g(T)}{\varphi_d(T)}. \quad (24)$$

Because of the additional geometric phase  $\varphi_g(T)$  leading to precession, the Compton frequency  $\omega$  is a little more than  $M = 137$  times the orbital Bohr frequency  $\omega_M$  of the electron. In the rolling cone picture, the ‘rolling’ Compton wave number or cone base radius rolling at distance  $R$  is given by  $\lambda = R'J/M = RJ\omega_M/\omega$ .

## Hypocycloidal and epicycloidal dynamics

Additionally to the coupling of dynamical phase and precession a radial resonance of geometric phase and precession angle could be induced, see fig.1. These resonances can be projected to a planetary gear model in plane showing hypocycloidal and epicycloidal dynamics with equivalent phase evolution, see fig.2. A counter-rotating hypocycloidal geometric phase (+) generates more dynamical sub-loops on the total loop than in the epicycloidal case (-). In the most simple case the total phase rotates by  $\pm 4\pi N$  while the geometric phase rotates by  $2\pi$ . Subtracting Berry’s phase from the total phase of one closed loop gives  $|N_{\pm}| = N \pm \frac{1}{2}$ , the total dynamical phase in the hypocycloidal and epicycloidal paths shows  $N_+ > 0$  and  $N_- < 0$  sub-loops, respectively. The correspondent quantum number  $N_{\pm}$  includes two cases labelled by the  $\pm$  sign of the geometric phase evolution with respect to the dynamical phase evolution with

$$-N_{\pm} = M \frac{\gamma\omega_M}{\omega_p} = \frac{\varphi_d(T)}{\varphi_{g\pm}(T)} = \frac{\varphi(T)}{\varphi_{g\pm}(T)} + 1. \quad (25)$$

The sign convention is adjusted to the sign of the charge and to  $|N_+| = |N_-| + 1$  for a given ratio of loop/sup-loop radius, by definition, the sign of  $N_{\pm}$  is opposite to the sign of  $M$  in eq.(10). Half integral values of the quantum number  $|N_{\pm}|$  in eq.(25) indicate an interference of the precession frequency with both, the orbital rotation and particle Compton frequency.  $-\varphi(T)/\varphi_g(T) = N_{\pm} - 1$  is known as the winding number on helical photon paths, note that according to eq.(9) Berry’s potential  $A$  is a winding number density. The number characterizes both, a standing wave in radial and orbital dimension. The ratio dynamical to total phase evolution is given by

$$\cos(\theta) = \frac{2N_{\pm} \mp 1}{2N_{\pm} \pm 1}, \quad (26)$$

where  $N_0 = |N_{\pm}| \mp \frac{1}{2} > 0$  is in the case of hypocycloidal and epicycloidal phase-locking the next higher available integral number with respect to the free running irrational number  $N$  based on  $M$  and  $M_g$  where  $-|N_{\pm}| > N_0$ , see table 1. The dynamical coupling strength for any  $N$  provides for the ratio

$$\left| \frac{\varphi_{d+}(T)}{\varphi_{d-}(T)} \right| = \frac{2N + 1}{2N - 1} = \frac{r_a + r_b}{r_a - r_b}, \quad (27)$$

where the circle of radius  $r_b$  rolls on or in the circle of radius  $r_a$ . Now there are two principle integral parameters  $M$  and  $N$  providing for single-valuedness on the closed loop, where  $N$  is a consequence of  $M$  in the case of hypocycloid/epicycloidal resonances.

## Charge

The modern interpretation of the fine-structure constant defines  $\alpha$  as the coupling constant for the electromagnetic force. Solving eq.(18) or eq.(19) by iteration provides for the balance of dynamical and geometric phase given by  $\alpha$  subject to a given number of sub-loops  $M$ , coupling

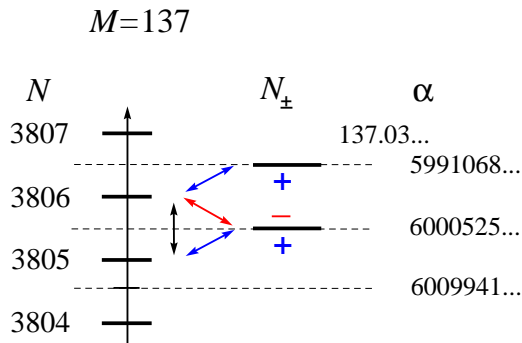


Figure 3: The  $N_{\pm}$  hypocycloidal or epicycloidal levels for the relevant  $N$ -values in the case  $M = 137$  where  $N_0 = 3806$ .

loops  $M_g$ , sub-loop spin  $J$ , and eventually  $N$  characterizing a hypocycloidal or epicycloidal resonance. The coupling is polar since a positive and negative  $M/M_g$  corresponds to the repulsive and attractive case, respectively, in the negative case the coupling phase interval and precession of eq.(17) is negative with respect to the total phase in eq.(10). Consequently, the hypocycloidal and epicycloidal character with negative and positive curvature can be assigned to a negative and positive coupling sign, respectively, see fig.2. In fig.2 it is shown how both types must be combined in circular symmetry: the positive charge must ‘roll’ inside as a hypocycloidal with  $N$ , and the negative charge outside as an epicycloidal with  $N + 1$  sub-loops. This could be helpful for an interpretation of nature’s symmetry breaking regarding positive and negative charges, especially ‘charged’ fine structure measurements with a shift based on  $|N_-| + 1 = |N_+|$ . Since  $M_g$  is a spin-independent coupling number and the effective coupling should be proportional to spin, it is straightforward to introduce  $Z_e = JM_g$  as a charge number. This enables to determine the same  $\alpha/J$  in eq.(18) for different  $Z_e$  since  $M/Z_e$  is  $\alpha$ -scale invariant and counts the sub-loops necessary to generate one basic coupling loop. As shown by Berry, a geometric phase is produced in the field of a magnetic monopole [1]. The geometrical phase in quantum mechanics is ultimately related to the construction of an Abelian monopole since this is the only topologically non trivial object which arises when the structure group is  $U(1)$ [6]. For electrodynamics, the gauge group is  $U(1)$  which has the topology of a circle, on which the homotopy classes of closed curves are labelled by their winding or loop numbers, and where the magnetic charge is quantized taking integral values [3]. The topological nature of the monopole charge is by definition discrete and invariant under continuous deformations. Dirac [3] showed that the existence of magnetic monopoles can explain the quantization of electric charge and that a monopole must carry a magnetic charge which is an integral multiple of  $68.5$ . According to these monopole properties and the  $U(1)$  relation to the Berry phase for  $J = \frac{1}{2}$ ,  $M = 137$  is the topological candidate to generate the quantum monopole charges of magnetism and electrostatics. All-in-all, it suggests to take  $\alpha_0 = \alpha(M = 137) = 1/137.036009412\dots$  as a candidate for the free or neutral Sommerfeld-Dirac fine structure constant, see tables 1 and 2. Variations are likely since external fields could force hypocycloidal or epicycloidal resonances depending on the polarity of the coupling. Spin-orbit coupling based on linear phase relations suggests to visualize precession by cones rolling in or on cones.

Visualizing Thomas precession and aberration (angle  $\theta$  obtained by infinitesimal Lorentz boosts) [14] already pointed out, that the geometric phase can be found in classical mechanics with a gyroscope or point-like compass as a solid-body turn during conical movement [15].



## Overload

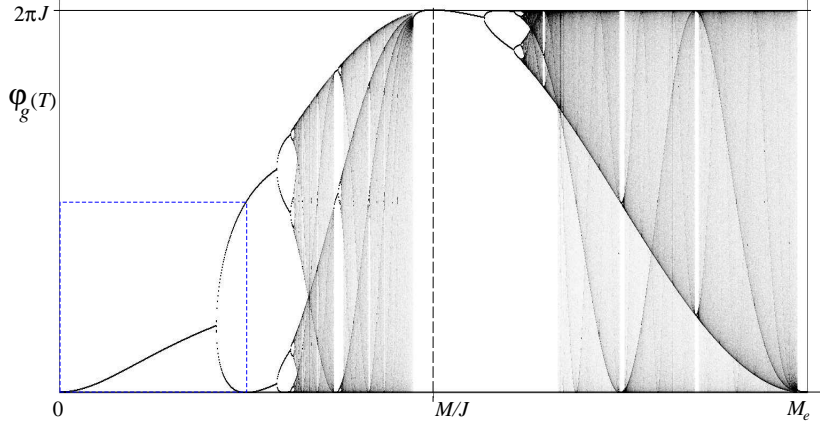


Figure 4: Chaotic occupation density of geometric phase space for a variable coupling number  $M_g = Z_e/J$ . Stable regions with one fixed  $\varphi_g(T)$ -value and bifurcations occur periodically. Stable regions for  $J = \frac{1}{2}$  and  $M = 137$  exist with  $M_g$  values 1-114, 260-310, 541-568. Feigenbaum's number  $\approx 4.669$  characterizes the branching sequence of bifurcations. The dashed blue rectangle shows  $M_g \leq 137$  for  $J = \frac{1}{2}$ .

Increasing  $|M_g/M|$  will increase the precession semiangle  $|\theta|$  for a given dynamical phase of the sub-loop  $\Delta\varphi_d(T)$ . With variable  $M_g$ , eq.(18) and eq.(19) characterize a complex one-dimensional system that can show chaotic dynamics and quasiperiodicity [16]. It is a cosine map related to the circle and sine map [17] and as an iterative system it shows asymptotic stable and converging regimes but also bifurcations and unstable regimes for special feedback coupling strengths  $M_g$ . The geometric part and precession will become more and more dominant with increasing  $M_g$ , blocking or occupying phase space as a charge-dependent screening effect, see fig.4. If the nonlinear system characterizes Coulomb coupling and fine structure, the chaotic dynamics should be found in charged nuclei where  $M_g$  reaches the critical value. Since the production cross section was found to be rapidly decreasing with the atomic number near 114 [18], it was concluded that it would be very difficult to reach still heavier elements. In fig.4 the first stable regions with one fixed  $\varphi_g(T)$ -value ends near  $M_g = 114$ , the next bifurcations occur periodically. This indicates, that the Coulomb coupling generating chaotic electrodynamics could to some extent be responsible for the instability of the nucleus.

## Measurement

Over the years there was a discussion about the value of the fine structure constant. Different values measured with comparable accuracy disagree in different directions by several standard deviations. The additional quantum condition eq.(26) selecting the hypocycloid or epicycloid character could force extra shifts  $\approx N^{-2}$ , for  $M = 137$  about  $3806^{-2} \approx 6.9 \cdot 10^{-8}$  (see table 1 and fig.3). Such shifts are likely to be observed in the charged case if the Compton wavelength couples to the precession frequency with asymmetry  $N \pm \frac{1}{2}$  in eq.(26). So it remains to check if measurements based on externally forced loops in modulated fields or internal forced loops due to mass-to-charge coupling could favor the correspondent resonances leading to hypocycloidal or epicycloidal phase evolutions. And there is a strong evidence regarding the probably most often cited and accurate measurements of the fine structure constant over the last years. It seems, that measurements can be grouped into three  $\alpha$ -categories:  $\alpha_0$ ,  $\alpha_-$ , and  $\alpha_+$ , see fig.5:

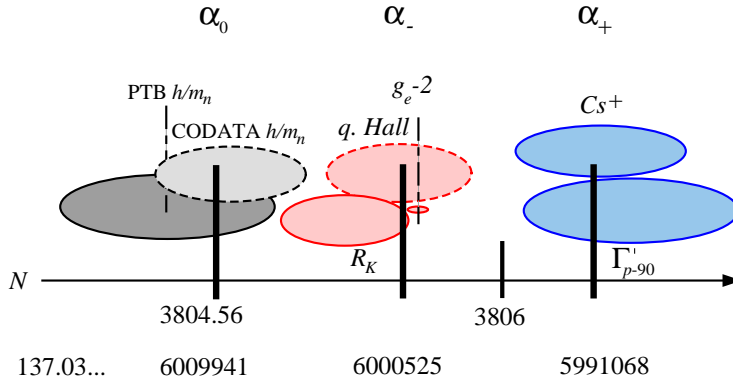


Figure 5: Regarding the most accurate measurements of the last years there is almost no overlap between the three different setups given by neutron (free running  $\alpha_0$ ), electronic (epicycloidal  $\alpha_-$ ), and protonic (hypocycloidal  $\alpha_+$ ) couplings. Dashed are combined values of different measurements.

- The free running value  $\alpha_0$  fits very well to  $h/m_n$  neutron experiments [19, 20]. The value is also supported by a CODATA  $h/m_n$  evaluation  $\alpha_0^{-1} = 137.0360084(33)$  [19] that is a combination of the PTB, IMGCC, and NRLM results. Over the years this range was confirmed by repeated PTB experiments providing for  $\alpha_0^{-1} = 137.03601144(498)$  [20, 21, 22, 23], see table 3. The neutron values have been obtained by measuring the de Broglie wave length of a beam of neutrons and the Bragg reflection in a perfect silicon crystal.
- The epicycloidal  $\alpha_-$  corresponds to measurement based on single electrons. The prominent electron  $g - 2$  value  $\alpha_-^{-1} = 137.03599958(52)$  in [24] fits within 5 ppb (relies on extensive QED calculations and does strongly contribute to the 1998 CODATA evaluation [25, 19, 26]), see table 3. To this type also fits the mean value  $\alpha_-^{-1} = 137.0360008(30)$  of two well known experiments obtained by the quantum Hall effect with  $\alpha_-^{-1} = 137.03599790(320)$  in [27] and  $\alpha_-^{-1} = 137.0360037(27)$  in [28]. The von Klitzing NIST-97 value  $R_K \alpha_-^{-1} = 137.0360037(33)$  [19] fits also to the electronic value.
- The protonic hypocycloidal  $\alpha_+$  was found with measurement error smaller 40 ppb [19] by the NIST-89 shielded proton gyromagnetic ratio  $\Gamma'_{p-90}(lo) \alpha_+^{-1} = 137.0359880(51)$ . A recent Penning trap value obtained with  $Cs^+$   $\alpha_+^{-1} = 137.0359922(40)$  [29] fits also very well, see table 3, but does not contribute to the CODATA recommended value [19].

## Conclusion

The probably most prominent fundamental constant can be within measurement uncertainty reproduced by iterative phase relationships that obey the single-valuedness requirement. If this paper provides for a correct approach to the nature of fine structure and charge, the strength and sign of coupling is controlled by Berry's phase. Especially the effect generated by the coupling sign is highly interesting, Berry's phase can evolve against or with the dynamical phase depending on the sign of curvature. Measuring the correspondent shifts could play a crucial role since they would indirectly confirm (a) the existence of magnetic monopoles and (b) the coupling of dynamical and geometric phase. The present experimental situation supports the proposals of this work, especially the relevance of hypocycloidal or epicycloidal resonances. There is a

Table 2:

A simple comparison matrix in standard deviation units  $\sigma_i$  comparing three different types of the most relevant measurements [24] based on neutron <sup>1</sup>, electron  $g - 2$  <sup>2</sup>, proton Cs<sup>+</sup> <sup>3</sup> measurements, see fig.5. The diagonal values indicate a significant correlation to the calculated values.

	137.03601144(498) <sup>1</sup>	137.03599976(50) <sup>2</sup>	137.03599220(400) <sup>3</sup>
137.03600941164 <sup>4</sup>	<b>-0.4</b> $\sigma_1$ / <b>-1.5</b> ·10 <sup>-8</sup>	+19 $\sigma_2$ /+7.0 ·10 <sup>-8</sup>	+4.3 $\sigma_3$ /+13 ·10 <sup>-8</sup>
137.03600052556 <sup>5</sup>	-2.2 $\sigma_1$ /-8.0 ·10 <sup>-8</sup>	<b>+1.5</b> $\sigma_2$ /+ <b>5.6</b> ·10 <sup>-9</sup>	+2.1 $\sigma_3$ /+6.0 ·10 <sup>-8</sup>
137.03599106791 <sup>6</sup>	-4.1 $\sigma_1$ /-15 ·10 <sup>-8</sup>	-17 $\sigma_2$ /-6.3 ·10 <sup>-8</sup>	<b>-0.3</b> $\sigma_3$ /- <b>8.3</b> ·10 <sup>-9</sup>

<sup>1</sup> 1998 Neutron value [20], <sup>2</sup> 1999 Codata approx. electron  $g - 2$  [19, 26], <sup>3</sup> Penning trap [29],

<sup>4</sup> free running solution of table 1, <sup>5</sup> 3805.5 resonance of table 1, <sup>6</sup> 3806.5 resonance of table 1

strong evidence that  $\alpha_0 = \alpha(M = 137)$  is a candidate for the Sommerfeld-Dirac fine structure constant. Without knowing the driving mechanism that leads to coupling and curvature beyond general relativity, single-valuedness of  $M$  on the closed path (and  $N$  subject to external fields) can guide to exact results governed by a number of physics relations that are:

- $\alpha_0$  is based on a plausible connection between the geometric and dynamical phase,
- the Berry phase screening  $1 - M\alpha_0/J$  of electrodynamic coupling provides the necessary magnetic monopole component to quantize charge,
- $\alpha_0$  is perfectly compatible with gravitomagnetic coupling,
- the correspondence principle is satisfied by ‘classical’ counterparts,
- chaotic dynamics and instability could fit to known instabilities of superheavy charged nuclei, see fig.4, outside the chaotic regime the coupling mechanism is flexible, self-consistent, regenerative, and self-balancing subject to external distortions,
- positive and negative curvatures and related sign in Berry’s phase requires to introduce  $\alpha_+$  and  $\alpha_-$  based on the hypocycloidal and epicycloidal character, respectively,
- based on  $N_0 = 3806$  the shifts  $\approx 3806^{-2} \approx 6.9 \cdot 10^{-8}$  are supported by highly rated measurements, see fig.5, where the epicycloidal  $\alpha_- \approx 1/137.03600052556$  with  $N_- = 3805.5$  fits within a view ppb to the indirect QED electron  $g - 2$  determination, the ‘free’ neutron measurements with  $\alpha_0 \approx 1/137.03600941164$  to  $N \approx 3804.56$ , and the proton dominated measurements to  $N_+ = 3806.5$  with  $\alpha_+ \approx 1/137.03599106791$ .

Spin-orbit coupling with coupled phase conditions (e.g. between a global and a local phase) can be found in many cyclic quantum systems, especially in highly symmetric or degenerated mesoscopic systems showing helical or regular  $M$ -polygonal structure. Spin precession of electrons in cyclic motion can lead to various interference phenomena such as oscillating persistent current and conductance [30]. For solids, atoms, or in nuclear physics it should be possible to define more complex and generalized fine structure constants that characterize the back reaction of the geometric phase to the dynamical phase for more complex paths, probably involving lattice interaction, especially in situations where interaction between vibrational and electronic states happens in the degenerate state (i.e. Jahn-Teller effect). In this case the phenomena of

superconductivity and bose-einstein condensates could probably also benefit from special feedback relationships between the geometric and dynamical phase, supported by regeneration and revival processes characterized by generalized fine structure constants. I suspect that the type of fine structure constants tabulated in table 1 could appear only in the simplest cases of one-dimensional systems, i.e. in fullerene rings or tubes or in Heisenberg spin chains, especially if neighboring units generate cooperative spin resonance phenomena. Although, the mathematics that leads to the number  $M = 137$  is open, topology and geometry in the  $\alpha$ -theory part of this work could guide experimentalists and theorists to new connections between electrodynamics and (loop-)gravity. Regarding the identical coupling relation predicted by gravitomagnetism, the tiny magnitude of the gravitomagnetic field in a classical measurement does not necessarily mean, that the magnitude of the emerging geometric phase and related quantum mass-energy currents in feedback loops must be tiny. A loop-gravitational gravitomagnetic field magnitude reaching the electromagnetic level would shift the Planck scale to the nuclear range. Regarding the  $\alpha$ -powers produced with  $N^2$

$$\alpha^2 \approx \frac{2}{\pi^2 N}, \quad (28)$$

the Berry contribution with coupling change  $\Delta\alpha/\alpha$  proportional to  $1/N^2$  has lowest order  $\alpha^4$ -terms. It should be interesting to note, that hyperfine, fine structure, and Lamb shift are usually assigned to the same  $\alpha$ -power dependency. But geometric phase contributions are totally missing in almost all QED evaluations of the atomic spectra.

## Summary

This article starts by a quick evaluation of the role and status of Berry's phase. Although, Berry's phase especially the Aharonov-Bohm phase can be related to a gauge potential that is very similar to a magnetic monopole potential, (hyper)fine structure and Lamb shift theories handling the most accurate measurements seem to ignore Berry's phase. The rather exotic status seems to imply for many scientists that Berry's phase could have no big impact on the quantum mechanics of atomic energy spectra. This is quite normal, since Berry's phase is quite young. To provide for examples that support the proposal of this article, Sommerfeld fine structure constant  $\alpha$  is successfully defined based on Berry's geometric phase coupling back to the hamiltonian-induced dynamical phase in a phase-locked spin-orbit system.  $\alpha$  identified as the ratio of orbital to Compton wave number fits exactly to gravitomagnetic interaction (general relativity). Moreover, the resulting nonlinear affine iteration  $\alpha = \cos(\pi\alpha)/M$  provides for a free running solution outside the chaotic regime, where the Berry phase screening component  $1 - M\alpha$  of electrodynamic coupling can be assigned to magnetic monopoles on  $SU(2)/U(1) = S^2$  with  $M = 137$  as required by Dirac. In the chaotic regime the onset of bifurcations could fit to known instabilities of superheavy charged nuclei. A sub-quantization of  $\alpha$  based on a integral winding number shows three basic categories of solutions: the free neutral value  $1/\alpha=137.03600941164$ , and the next protonic (hypocycloidal) and electronic (epicycloidal) resonances at 137.03599106791 and 137.03600052556, respectively. This could resolve the disagreement of  $\alpha$ -values obtained by different measurements using neutrons, electronic, and protonic interactions. Almost all of the current available, most accurate, and most often cited measurements and evaluations of  $\alpha$  fit within standard deviation (a view ppb's) to the correspondent values. The results of this article shows, that it possible to built a bridge via Berry's phase between classical physics, quantum electrodynamics, and general relativity and that the exotic status of Berry's phase has to be replaced by the probably most fundamental status of mathematical physics.

## References

- [1] M. V. Berry, Proc. Roy. Soc. Lond. A **392**, 45 (1984).
- [2] R. Batterman, ‘Falling Cats, Parallel Parking, and Polarized Light’ (2002); PITT-PHIL-SCI00000583.
- [3] P. A. M. Dirac, Proc. Roy. Soc. London A **133**, 60 (1931).
- [4] Y. Aharonov, J. Anandan, ‘Phase Change During a Cyclic Quantum Evolution’, Phys. Rev. Lett. **58**, 1593 (1987).
- [5] D. Suter, K. T. Mueller, A. Pines, Phys. Rev. Lett. **60**, 1218 (1988);
- [6] F.V. Gubarev, V.I. Zakharov, Int. J. Mod. Phys. **A17**, 157 (2002); hep-th/0004012.
- [7] B. Binder, alpha simulation; <http://www.quanics.com/spinorbit.html>
- [8] B. Mashhoon, Gen. Rel. Grav. **31**, 681-691 (1999); gr-qc/9803017.
- [9] I. Ciufolini, J. A. Wheeler, “Gravitation and Inertia”, Princeton University Press, Princeton, New Jersey, (1995).
- [10] B. Mashhoon, R. Neutze, M. Hannam, G. E. Stedman, Phys. Lett. A **249**, 161-166 (1998); gr-qc/9808077.
- [11] B. Mashhoon, F. Gronwald, F.W. Hehl, D.S. Theiss, Ann. Phys. **8**, 135 (1999); gr-qc/9804008.
- [12] Gravity probe B experiment homepage  
F. Everitt, Stanford.
- [13] A. Camacho, ‘Coupling gravitomagnetism-spin and Berry’s phase’;  
gr-qc/0206005.
- [14] G. B. Malykin, G. V. Permitin, “Thomas precession”, in Physical Encyclopedia 5, 108 (1998).
- [15] A. Ishlinski (Mechanics of Special Gyroscopic Systems, Kiev: Izd. AN USSR, 1952).
- [16] M. J. Feigenbaum, L. P. Kadanoff, S. J. Shenker, Physica D **5**, 370, (1982).
- [17] R. L. Devaney, An Introduction to Chaotic Dynamical Systems, Redwood City, Addison-Wesley, (1987).
- [18] P.H. Heenen, W. Nazarewicz, Europhys. News **33**, No. 1 (2002)  
<http://www.europhysicsnews.com/full/13/article2/article2.html>.
- [19] P. J. Mohr, B. N. Taylor, Rev. of Mod. Phys., **72**, No. 2, 351 (2000).
- [20] E. Krüger, W. Nistler, W. Weirauch, Metrologia **36**, 147 (1999).
- [21] E. Krüger, W. Nistler, W. Weirauch, Metrologia **22**, 172 (1986).
- [22] E. Krüger, W. Nistler, W. Weirauch, Metrologia **32**, 117 (1995).
- [23] E. Krüger, W. Nistler, W. Weirauch, Metrologia **35**, 203 (1998).
- [24] T. Kinoshita, ‘Everyone makes mistakes - including Feynman’, (2001); hep-ph/0101197.
- [25] P. J. Mohr, B. N. Taylor, Physics Today **54**, 29 (2001);  
Physics Today March (2001) online.
- [26] M. S. Dewey, E. G. Kessler Jr., J. Res. Natl. Inst. Stand. Technol. **105**, 11 (2000).
- [27] M. E. Cage et al., IEEE Trans. Instrum. Meas. **38**, 284 (1989).
- [28] A. Jeffery et al., IEEE Trans. Instrum. Meas. **46**, 264 (1997).
- [29] M. P. Bradley et al., Phys. Rev. Lett. **83**, 4510 (1999).
- [30] Y.-S. Yi, T.-Z. Qian, Z.-B. Su, Phys. Rev. B **55**, 10631 (1997);  
cond-mat/9705054.